Journal of Geochemical Exploration 152 (2015) 1–9

Contents lists available at ScienceDirect

Journal of Geochemical Exploration

journal homepage: www.elsevier.com/locate/jgeoexp

Elemental distribution in the topsoil of the Lake Qinghai catchment, NE Tibetan Plateau, and the implications for weathering in semi-arid areas

Ping Wang [a,b], Junji Cao [a,b,c,*], Yongming Han [a,b,**], Zhangdong Jin [b], Feng Wu [a,b], Fei Zhang [b]

[a] Key Lab of Aerosol Chemistry & Physics, Institute of Earth Environment, Chinese Academy of Sciences, Xi'an, China
[b] State Key Lab of Loess and Quaternary Geology, Institute of Earth Environment, Chinese Academy of Sciences, Xi'an, China
[c] Institute of Global Environmental Change, Xi'an Jiaotong University, Xi'an, China

ARTICLE INFO

Article history:
Received 20 April 2014
Accepted 11 December 2014
Available online 20 December 2014

Keywords:
Topsoil types
Chemical index of alteration
GIS mapping
Human influence

ABSTRACT

An understanding of topsoil geochemistry within a watershed helps to identify the influence of natural processes and anthropogenic activities in the environment. Fifteen elements were measured in 73 topsoil samples (top 30 cm) from the Lake Qinghai catchment, NE Qinghai–Tibetan Plateau (QTP) in 2009, to investigate geochemical patterns, identify possible sources and explore the implications of chemical weathering. Compared with their content in the upper continental crust (UCC), a deficit of Cu and Zn and an enrichment of Pb were identified in the study area. Enriched Ca levels were observed in alpine soil and pedocal, solonchak and aeolian sand soils, whereas there was a loss in hydromorphic and semi-hydromorphic soils. High Na in marsh solonchak indicated the possible presence of evaporites. Cluster analysis (CA) and principal component analysis (PCA) indicated the dominance of carbonate and the accumulation of P, possibly from grassland litterfall in topsoil. Some human activities have exerted an influence on virgin topsoil, as revealed by GIS mapping. The implications for chemical weathering, based on a chemical index of alteration (*CIA*) and an Al_2O_3–($CaO^* + Na_2O$)–K_2O (A–CN–K) diagram were characterised by a major carbonate control of the primary weathering stage under cold-dry climatic conditions with Ca and/or Na removal.

1. Introduction

The geochemistry of major and trace elements in topsoil can be used to determine the geochemical significance, rock weathering properties and anthropogenic influences in drainage basins. Studies of watershed geochemical characteristics resulting from supergene geologic processes have therefore long been of scientific interest (Angelone et al., 1993; Baveye et al., 2011; Li and Yang, 2010). Numerous geochemical investigations of topsoil have been undertaken in recent decades in areas such as Europe (Korobova et al., 1997; Peltola and Astrom, 2003), America (Almeida et al., 2005; Larney et al., 1995), Oceania (Lottermoser et al., 1999), Africa (Olorundare et al., 2011) and Asia (Qiu et al., 2014; Yang et al., 2010).

In China, the quantitative data regarding trace element levels in topsoils have been used to estimate the heavy metal concentrations in soils (Li et al., 2012), to explore the mobility, bioavailability, and human bioaccessibility of different trace metals (Luo et al., 2012a), to obtain the fluxes of soil heavy metal input/output pathways (Xia et al., 2013), to identify possible sources using multivariate statistical analysis (cluster analysis (CA) and principal component analysis (PCA)), GIS mapping techniques, or Pb isotopic composition analysis (Facchinelli et al., 2001; Wong and Li, 2004), and to investigate the potential risks to ecosystems and human health (Li et al., 2014; Wei and Yang, 2010). The levels of major elements were generally dependent on the lithology of the soil parent material and the pedological processes responsible for the formation of soils (Baize and Sterckeman, 2001). The chemical index of alteration (*CIA*) was based on the content of the major elemental oxides and has been used to compare the degree of soil formation (Nesbitt and Young, 1982), and an A–CN–K diagram (Al_2O_3–($CaO^* + Na_2O$)–K_2O) could reflect the changes in the principal components of chemical weathering processes in soil (Liu, 2009). In recent decades, these methods have been used in studies of urban soil (Luo et al., 2012b), street dusts (Han et al., 2008; Li et al., 2001), agricultural and non-agricultural soils (Liu et al., 2013; Sun et al., 2013), flood zones (Li and Zhang, 2010; Ye et al., 2011), human-constructed soils (Acosta et al., 2011), and mining and developed areas (Li et al., 2014; Teng et al., 2010). However, few studies have been undertaken to investigate the contaminated/uncontaminated conditions of the topsoil of the Lake Qinghai catchment.

Lake Qinghai, in the northeastern margin of the QTP, was located at the point of transition from an arid to semiarid climate zone. The area

* Correspondence to: J. Cao, Key Lab of Aerosol Chemistry & Physics, Institute of Earth Environment, Chinese Academy of Sciences, Xi'an, China.
** Correspondence to: Y. Han, State Key Lab of Loess and Quaternary Geology, Institute of Earth Environment, Chinese Academy of Sciences, Xi'an, China.
E-mail addresses: cao@loess.llqg.ac.cn (J. Cao), yongming@ieecas.cn (Y. Han).

http://dx.doi.org/10.1016/j.gexplo.2014.12.008
0375-6742/

has a harsh environment, sparse population and was experiencing degeneration and desertification of the grassland as a result of overgrazing. Qinghai Lake was a globally important wetland and an important area for the conservation of biological diversity (Wang et al., 2011). The Qinghai–Tibet railway passes along the lakeshore, and herdsmen settlements were located on both sides of a major road, the Qinghai–Tibet highway (Fig. 1). The natural and anthropogenic conditions make Lake Qinghai particularly suitable for scientific research due to its sensitivity to the environment. Previous studies of Lake Qinghai have focused on the reconstruction of the paleoenvironment and paleoclimate (Henderson and Holmes, 2009), hydrological and solute budgets (Jin et al., 2010b), changes in the lake water level (Li et al., 2007), and an investigation of the ecology (Cao and An, 2010). However, little was known about the elemental geochemistry of the topsoil in Qinghai Lake catchment.

The main objectives of this study were: (1) to investigate the native major- and trace-element content of different types of topsoil; (2) to identify possible sources of contamination and the spatial pattern of contaminant levels using multivariate analyses and GIS mapping techniques; and (3) to investigate the chemical weathering of the topsoil within the Lake Qinghai catchment. The results can be used to assess the topsoil contaminated/uncontaminated conditions and to provide better management of the Lake Qinghai catchment.

2. Materials and methods

2.1. Study area and topsoil types

The Lake Qinghai (36°32′–37°15′ N, 99°36′–100°47′ E, 3194 m a.s.l.) catchment, with a surface water area of 4260 km^2 and a water volume of 7.16×10^{10} m^3, was surrounded by four mountain ranges, namely the Riyue Mountains to the east, the Qinghai Nanshan Mountains to the south, the Shule south Mountains to the northwest, and the Datong Mountains to the north. Mountains with an elevation above 4000 m, account for ~70% of the drainage area. The climate was controlled by the Asian summer monsoon and westerlies, with strong solar radiation and long, cold winters, and short, cool summers. Frost can occur at any time of the year (Yu and Zhang, 2008). The mean annual air temperature (MAT) (1951–2007) was ~1.2 °C. The mean annual precipitation (MAP) (1951–2007) was 357 mm, but lake evaporation was 3–4 times higher than precipitation (LIGCAS, 1994). The bed rocks of the catchment consist of late Paleozoic marine sedimentary rocks that were composed primarily of limestone and sandstones, and a small amount of igneous rocks composed of granite, diorite and granodiorite. Quaternary loess was distributed around the lake, and the seasonally frozen earth was widely distributed in the valleys of the catchment (LIGCAS, 1979).

Based on the data from China's second national soil survey, the soil types in the study region were classified into the six soil orders and ten soil groups shown in Fig. 1. A soil classification benchmark system was established based on the genetic soil classification of China (GSCC), Staff (1999) (ST) and the World Reference Base for Soil Resources (WRB) (IUSS Working Group WRB, 2006). Alpine soil (including alpine frost desert soil, alpine meadow soil, and alpine steppe soil), pedocal (including chernozem and chestnut soil) and semi-hydromorphic soil (including mountain meadow soil) were zonal. They were mostly affected by altitude, precipitation and relief. However, hydromorphic (including bog soil and peat soil), solonchak (including marsh solonchak) and aeolian sandy soil were intrazonal. They were mainly affected by relief, depression and aeolian dust in the study area (Ma, 1997).

2.2. Sampling and chemical analyses

A total of 73 surface soil samples (0–30 cm depth, after removing grass turf) were taken from the Lake Qinghai catchment during 1 July–30 September 2010 (Fig. 1). About 1 kg of each soil sample was collected using a stainless steel spade and a plastic scoop, and fresh

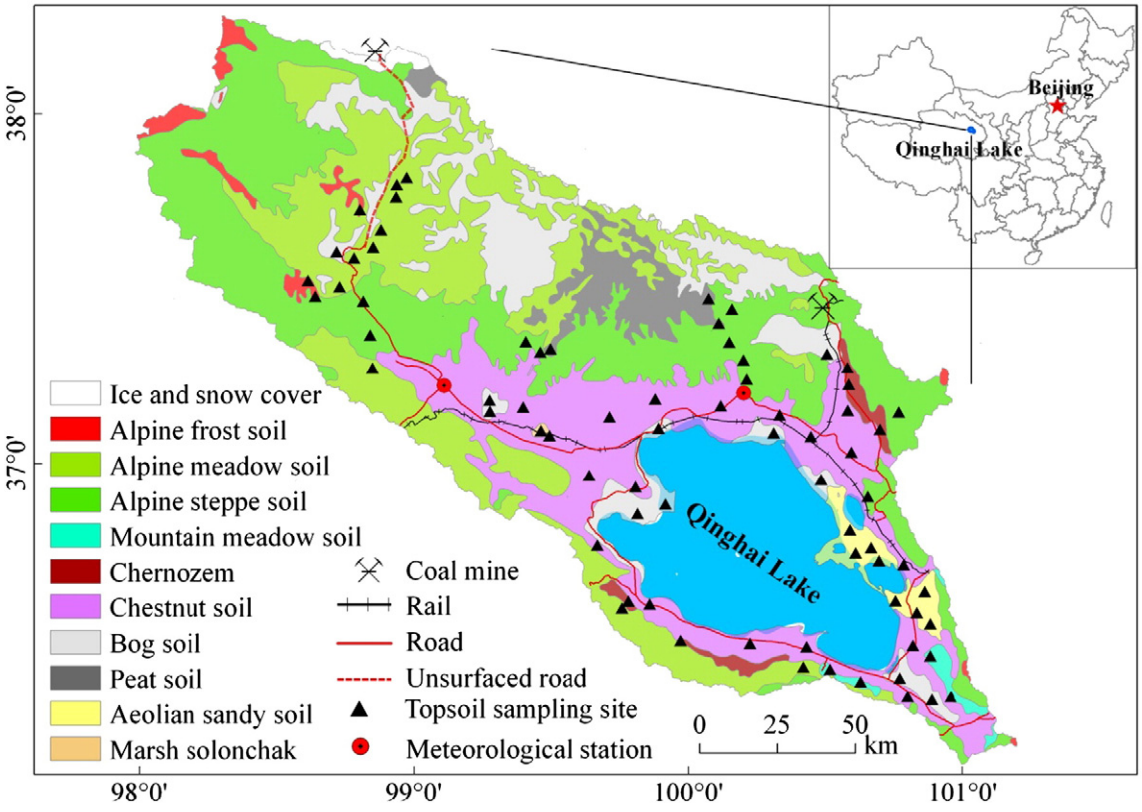

Fig. 1. Topsoil types and distribution of sampling sites within the Lake Qinghai catchment.

samples were placed in food bags. The coordinates of the sampling locations were recorded with a differential GPS. All samples were freeze-dried, then ground to pass through a 200-mesh sieve (<74 μm) and homogenised in an agate mortar. Five grams of the powdered sample were compressed into a thin compact disc (approximately 3.2 cm in diameter). The concentrations of 15 elements in bulk topsoil (Ca, Na, Mg, K, Al, Si, Fe, P, Ti, Cu, Zn, Pb, Rb, Sr and Zr) were measured using Energy Dispersive X-Ray Fluorescence (ED-XRF) spectrometry (Epsilon 5 ED-XRF: PANalytical B.V., The Netherlands). Calibration was undertaken using national reference samples (15 soil samples (GSS 1–7 and 9–16) and 11 stream sediment samples (GSD 1–11)). Analytical precision, as verified by replicate analyses of GSS-8, was better than 1% for the major elements and better than 5% for trace elements.

2.3. Multivariate analysis and the GIS mapping technique

Principal component analysis was widely used to extract a small number of latent factors (principal components, PCs) when analysing relationships among observed variables (Loska and Wiechuła, 2003). To make the results more easily interpretable, the VARIMAX normalised rotation of PCA was also applied to maximise the variances of the factor loadings across the variables for each factor. Generally, factor loadings >0.72 were regarded as excellent and <0.33 were regarded as very poor. In this study, all principal factors extracted from the variables were retained with eigenvalues >1.0, as suggested by the Kaiser criterion (Kaiser, 1960). When the VARIMAX normalised rotation of PCA was performed, each PC score contained information for all of the elements within a single number, while the loadings showed the relative contribution of each element to that score.

Cluster analysis was performed to further classify elements with different sources on the basis of the similarities of their chemical properties. In this study, hierarchical cluster analysis was used to identify relatively homogeneous groups of variables. The algorithm used began with each variable in a separate cluster and combined the clusters until only one was left. As the variables had large differences in scaling, standardisation was performed before computing the proximities. These steps can be performed automatically by the hierarchical cluster analysis procedure. A dendrogram was constructed to assess the cohesiveness of the clusters formed, in which correlations among elements can readily be seen (Han et al., 2006).

Cluster analysis was complementary to principal component analysis. PCA and CA were the most common multivariate statistical methods used in environmental studies (Diaz et al., 2002; Han et al., 2006).

The GIS mapping technique was used to produce spatial distribution maps for some elements in topsoil. To obtain the overall patterns of these elements, the spatial interpolation method of inverse distance weighting (IDW) was applied for 12 neighbouring samples that were used for the estimation of each grid point. The geochemical maps that were obtained were then overlaid with other thematic maps such as road systems, railways, villages and mining sites (Rishui and Muli coalfield) using ArcGIS 10.0 software. GIS was used in this study for the following: (a) to locate the sampling locations, (b) to generate geochemical maps showing hot-spots of some elemental concentrations in topsoil, and (c) to analyse the correlation between elevated levels of elements in topsoil and road networks, railways, locations of villages and mining sites, and even landscapes using GIS spatial overlay analysis techniques (Li et al., 2004).

2.4. CIA calculation and the A–CN–K diagram

The chemical index of alteration has been extensively applied as a proxy to examine weathering (Nesbitt and Young, 1982). The *CIA* value was defined as:

$$CIA = \frac{Al_2O_3}{(Al_2O_3 + CaO^* + K_2O + Na_2O)} \cdot 100 \quad \text{(Molar proportions)}. \quad (1)$$

Each oxide denotes the molar content, where CaO^* represents the CaO content of silicate minerals only and excludes the CaO combined in carbonate and phosphate minerals (Nesbitt and Young, 1982). Because it was difficult to accurately separate silicate minerals from the bulk samples, two methods were used to indirectly calculate the content of CaO^* in silicate minerals. Previous studies have shown that 1 mol/L HCl can effectively dissolve carbonate, phosphate, some authigenic Fe–Mn oxide minerals and a small amount of clay minerals such as chlorite (Shao and Yang, 2012). The CaO content in the residue fraction was then used for the *CIA* calculation. In addition, many studies using the *CIA* do not use an acid leaching method to remove non-silicate minerals, but rather adopt the correction method proposed by McLennan (1993), which suggests that CaO^* can be estimated by assuming reasonable Ca/Na ratios in silicate material. In Eq. (1), if $CaO > Na_2O$, $m_{CaO^*} = m_{Na2O}$ and if $CaO < Na_2O$, $m_{CaO^*} = m_{CaO}$. In this study, McLennan's method was applied to calculate the CIA values.

An Al_2O_3–($CaO^* + Na_2O$)–K_2O ternary diagrams based on the mass-balance principle, feldspar leaching experiments and the thermodynamic calculation of mineral stability has been used to predict the trend of continental chemical weathering and the alteration of mineralogical or geochemical components (Chen et al., 2001; Nesbitt and Young, 1982). The trend line from UCC to common shale in eastern China represents a typical early stage of continental chemical weathering.

3. Results and discussion

3.1. Concentrations of major and trace elements

A statistical summary of the major elements (K, Na, Ca, Mg, Al, Si and Fe) and trace elements (P, Ti, Cu, Zn, Pb, Rb, Sr and Zr) was given in Table 1. The mean values of these major elements were similar to the background values of soil in Qinghai (Ma, 1997). Compared with the UCC, Ca and Mg were enriched whereas levels of Na, K, Al, Fe and Si were lower than in the UCC (Chi and Yan, 2007). The ratios between the major elements (K, Na, Ca, Mg, Al, Si and Fe) in this study and those in the UCC were 1.5, 1.1, 0.5, 0.64, 0.75, 0.68 and 0.75, respectively. This was probably due to eluviation and the accumulation of alkaline earth elements (Ca and Mg), which dominated the carbonate weathering in this region. In relation to soil age, the leachability of Si, Fe and Al varied with the extent of weathering, with Si leached almost completely at the primary weathering stage, Fe at the secondary stage and Al at the advanced stage (Nesbitt and Young, 1984). The maximum loss was observed for alkaline elements (Na and K), although immobile elements (Al, Fe and Si) were also lost to some extent during soil genesis. In addition, exposed bedrock was located on the steep mountains (>3500 m a.s.l.), and thin layers of soil (<50 cm) that developed on the benchland on both sides of Qinghai lake tributary were present in the study area (Ma, 1997). It was this eluviation (A soil horizon, topsoil sampling sites) and accumulation (B horizon, no sampling data) of carbonate in the rock weathering processes that was the main factor affecting soil element geochemistry in the Lake Qinghai catchment. This was consistent with previous studies in the arid and semi-arid areas of the Tianshan Mountains of Xinjiang (Huang and Gong, 2005) and the unpopulated Kekexili region of the QTP (Huang et al., 2006).

The background values of trace elements in topsoil were important for the assessment of soil fertility and contamination status (Li et al., 2008; Teng et al., 2010; Yuan et al., 2014). Compared to the mean values of soils in Qinghai (Table 1), soils in the catchment were lower in Cu (16.83 mg/kg), Zn (54.26 mg/kg), Pb (17.39 mg/kg), Rb (86.3 mg/kg), Sr (204.94 mg/kg), and Zr (206.65 mg/kg) on average, but not Ti (3226.98 mg/kg) and P (missing P background data). The ratios between the trace elements measured here and those in the soils of Qinghai were 0.76, 0.68, 0.6, 0.85, 0.97, 0.97 and 1.01, respectively. The results clearly indicated a deficit of some trace elements (such as

Table 1
Chemical compositions (average concentration ± standard deviation) of various topsoils within the Lake Qinghai catchment.

Topsoil type	N[a]		Na (g/kg)	K (g/kg)	Ca (g/kg)	Mg (g/kg)	Al (g/kg)	Si (g/kg)	Fe (g/kg)	P (mg/kg)	Ti (mg/kg)	Cu (mg/kg)	Zn (mg/kg)	Pb (mg/kg)	Rb (mg/kg)	Sr (mg/kg)	Zr (mg/kg)
Alpine frost desert soil	3	AV[b]	1.03	2.26	11.00	1.49	6.86	26.07	3.82	905.46	3965.03	27.60	83.68	24.47	116.86	155.53	196.60
		SD[c]	0.05	0.33	0.40	0.39	0.12	1.72	0.74	169.67	422.39	5.83	12.79	3.75	13.43	35.01	18.86
		RSD[d]%	3.60	12.13	2.60	15.73	0.93	3.08	13.58	18.74	10.65	21.12	15.28	15.32	11.49	22.51	9.59
Alpine meadow soil	10	AV	1.39	1.73	5.28	1.50	6.23	22.27	2.70	768.61	3369.55	16.73	54.35	16.29	88.18	183.78	210.52
		SD	0.29	0.17	0.28	0.36	0.89	3.67	0.69	145.39	415.29	3.91	10.29	1.79	11.08	28.16	16.96
		RSD%	15.51	8.17	3.79	14.40	7.56	7.69	17.92	18.92	12.32	23.37	18.93	10.99	12.57	15.32	8.06
Alpine steppe soil	10	AV	1.65	1.49	7.56	1.20	5.25	23.98	1.88	562.11	2575.50	11.17	36.36	12.92	68.80	221.30	173.61
		SD	0.44	0.25	0.72	0.57	1.13	10.34	0.66	214.78	588.48	5.09	11.35	3.13	12.73	59.98	33.99
		RSD%	19.82	13.89	6.80	28.50	11.39	20.12	24.54	38.21	22.85	45.57	31.22	24.23	18.50	27.10	19.58
Mountain meadow soil	4	AV	1.62	1.73	2.84	2.09	6.09	23.64	2.49	630.77	3074.06	15.27	53.68	15.14	81.55	221.08	176.39
		SD	0.27	0.33	0.42	1.39	1.53	3.06	0.93	138.59	505.53	7.02	18.95	4.39	20.26	55.98	30.25
		RSD%	12.33	15.87	10.55	39.83	13.29	6.04	26.12	21.97	16.45	45.97	35.30	29.00	24.84	25.32	17.15
Chernozem	5	AV	1.37	1.71	3.11	1.67	6.14	20.83	2.70	750.00	3269.14	16.89	53.28	15.44	85.69	225.58	199.26
		SD	0.15	0.16	0.10	0.35	0.62	1.78	0.44	94.11	235.61	2.21	7.70	1.98	8.81	50.03	14.23
		RSD%	8.11	7.77	2.29	12.54	5.35	3.99	11.43	12.55	7.21	13.08	14.45	12.82	10.28	22.18	7.14
Chestnut soil	18	AV	1.34	1.88	4.61	1.48	6.09	23.85	2.81	804.01	3443.34	18.20	59.16	19.67	90.51	203.00	226.46
		SD	0.21	0.33	0.25	0.42	0.78	4.58	0.86	110.49	446.85	5.75	14.65	4.69	15.23	43.20	43.52
		RSD%	11.67	14.54	3.87	17.07	6.78	8.96	21.39	13.74	12.98	31.59	24.76	23.84	16.83	21.28	19.22
Bog soil	10	AV	1.60	1.69	1.93	1.17	5.28	28.35	2.04	617.22	2801.89	13.05	43.92	16.48	74.54	213.42	217.38
		SD	0.19	0.24	0.06	0.46	0.71	8.28	0.48	129.94	391.79	4.28	9.20	3.10	10.42	27.82	55.00
		RSD%	8.84	11.76	2.22	23.59	7.11	13.63	16.44	21.05	13.98	32.80	20.95	18.81	13.98	13.04	25.30
Peat soil	3	AV	1.19	2.38	2.46	1.36	6.81	27.33	3.70	877.15	3993.1	26.67	79.03	24.98	115.73	149.53	218.6
		SD	0.24	0.1	0.3	0.24	0.53	2.11	0.5	78.44	181.47	2.57	7.05	1.78	7.63	12.9	17.72
		RSD%	14.91	3.48	8.72	10.62	4.12	3.6	9.45	8.94	4.54	9.64	8.92	7.13	6.59	8.63	8.11
Marsh solonchak	2	AV	2.29	1.95	8.26	1.54	6.02	31.31	3.7	539.62	2906.85	17.78	47.92	15.91	80.28	270.1	175.58
		SD	0.08	0.48	1.44	0.57	0.13	0.41	0.47	35.48	12.43	0.93	0.91	0.46	1.81	2.23	13.19
		RSD%	2.6	20.43	12.46	22.18	1.14	0.61	12.7	6.57	0.43	5.23	1.9	2.89	2.25	0.83	7.51
Aeolian sandy soil	8	AV	1.28	1.78	4.05	1.66	6.50	21.82	2.95	763.88	3473.71	18.42	60.6	17.54	92.87	206.72	211.95
		SD	0.14	0.09	0.18	0.3	0.53	2.54	0.34	114.88	256.03	2.97	4.33	1.02	7.4	50.27	30.83
		RSD%	8.14	4.19	3.17	10.87	4.32	5.43	8.06	15.04	7.37	16.12	7.15	5.82	7.97	24.32	14.55
Sum	73	AV	1.47	1.86	5.11	1.52	6.13	24.94	2.77	1.47	3226.98	16.83	54.26	17.39	86.3	204.94	206.65
		SD	0.38	0.34	3.11	0.61	1.22	7.69	0.96	167.52	560.28	5.98	15.79	4.37	16.91	46.29	39.13
		RSD%	19.59	15.74	46.7	25	10.78	14.79	25.6	23.18	17.36	35.53	29.1	25.13	19.59	22.59	18.94
		Minimum	0.99	1.17	1.87	0.48	4.30	13.38	1.13	307.14	1690.89	3.95	19.34	8.04	49.17	119.63	108.88
		Maximum	2.32	2.46	11.26	3.28	7.07	33.12	4.13	1114.5	4241.3	31.4	94.2	27.24	125.3	354.46	347.4
		Skewness	1.12	0.35	0.98	1.39	−0.65	0.31	−0.1	−0.23	−0.64	−0.06	−0.02	0.4	−0.01	0.94	0.87
		Kurtosis	1.2	0.17	0.91	7.72	−0.31	0.72	−0.15	0.01	0.22	0.12	0.06	−0.17	0.03	0.99	2.49
Upper continental crust[e]			2.89	2.80	3.00	1.33	8.04	35.93	3.50		3000	25	71	17	112	350	190
Soils in Qinghai[f]			1.25	1.66	3.79	1.18	6.10		2.85		3200	22.2	80.3	29	102	212	214
Ratio to soils	UCC		0.51	0.67	1.70	1.14	0.76	0.69	0.79		1.08	0.67	0.76	1.02	0.77	0.59	1.09
	Qinghai		1.18	1.12	1.35	1.28	1.00		0.97		1.01	0.76	0.68	0.6	0.85	0.97	0.97

[a] N = sampling number.
[b] AV = average concentration.
[c] SD = standard deviation.
[d] RSD = relative standard deviation.
[e] Data from abundance of chemical elements of the UCC: a new table (Taylor, 1964).
[f] Data from soil in Qinghai (in Chinese) (Ma, 1997).

Cu and Zn) in the Lake Qinghai catchment, which was consistent with previous studies. Suo et al. (2000) found lower average concentrations of Cu and Zn (8.42 and 41.8 mg/kg) in plants than in soil (22.2 and 80.3 mg/kg), based on specimens of 46 plant species collected from the Qinghai Lake region. Similar levels to the mean values in the UCC were observed, except for a higher Pb level (17.39 mg/kg, corresponding to ratio of 1.02) (Table 1). The high Pb values in this catchment may have resulted not only from mining, but also from other causes such as atmospheric deposition. Dai et al. (2012) reported that the mining of coal deposits from the Early and Middle Jurassic (J_{1-2}) coal-forming periods might have generated the high Pb levels in topsoil (mean concentration of 16.64 mg/kg). Alternatively, Jin et al. (2009) recorded excess anthropogenic Pb in two short north–south sediment cores of the lake after subtracting lithogenic Pb, which was claimed to have been transferred to the lake and its sediments predominantly via atmospheric deposition. The high background values of Pb clearly require further investigation. The ratio of topsoil/UCC for P exceeded unity, suggesting an external input of P in topsoil, such as litterfall from grasslands, but not by the application of phosphate fertilizers in grassland (Zhao et al., 2007). Moreover, previous studies have indicated that P tends to be strongly absorbed by the soil colloids and accumulates in the surface horizon (Kleinman et al., 2003). It was fixed in surface soils and does not normally accumulate in sub-soils (Baker et al., 1975; Zhao et al., 2007). Finally, the weathering patterns of elements were constrained to the chemical characteristics of the element itself and the properties of element-bearing minerals. Minerals enriched in Rb (mica, potassium feldspar) were usually more weather-resistant than those enriched in Sr minerals (plagioclase, calcite and dolomite) under the same surface chemical weathering (Goldich and Gast, 1996). In addition, the Rb ionic radius was larger than that of Sr, and Rb was easily adsorbed on clay minerals. In contrast, Sr leaches easily and was lost (Nesbitt and Young, 1984). These differences in affinity for clay minerals would explain the observed variations.

Generally, the geochemical patterns of the major elements indicated that changes in the Ca concentration dominated the rock weathering processes, while there was a deficit of Cu and Zn, and enrichment of Pb and P.

3.2. Major elements in different topsoil groups

The elemental compositions normalised by the UCC in each topsoil group were shown in Fig. 2. Enriched Ca levels were observed in alpine

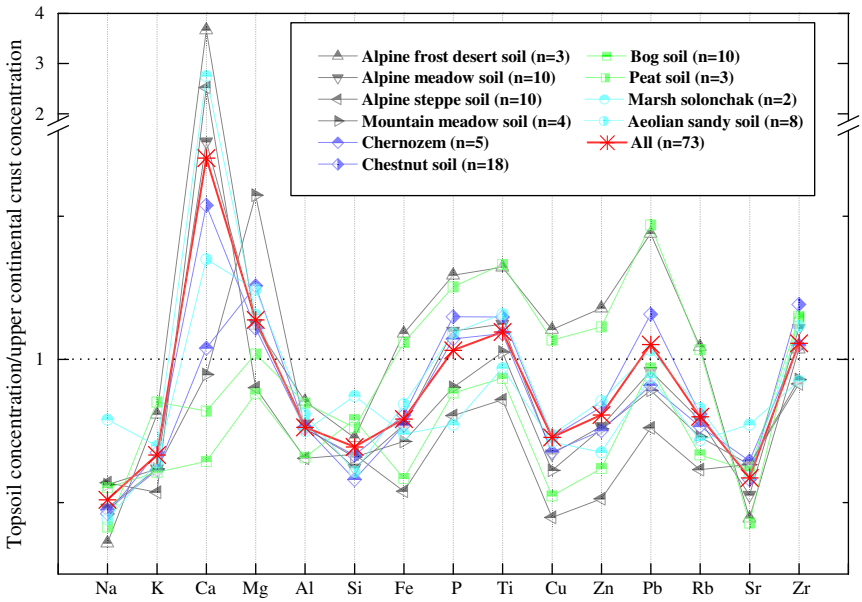

Fig. 2. Elemental compositions of topsoil groups normalised by upper continental crust.

soil, pedocal, solonchak and aeolian sand soil, whereas there was a loss in hydromorphic and semi-hydromorphic soils. Carbonates were dominant (Jin et al., 2010a) in alpine soils (15.4 ± 0.4% in alpine frost desert soil and 10.6 ± 0.7% in alpine steppe soil) that were distributed at high altitudes (3700–4200 m). Shattering and cracking under freeze–thaw and exfoliation all the year round may result in a calcium content in topsoil that was equivalent to that of bedrock (ISSCAS, 1978). Aeolian sandy soil at low latitudes (3000–3400 m) was deposited at the northeast shore of the lake. Previous studies have suggested that aeolian sediments originate from the Qaidam Basin in the adjacent northern QTP (An et al., 2012; Qiang et al., 2010), with a dominance of Ca–Al–Si in the lake sediments and loess in the Lake Qinghai catchment. However, the Ca content of hydromorphic and semi-hydromorphic soils was located in depression, and was easily lost in soil freezing–thawing processes (Wang et al., 2013).

Compared to the other groups, marsh solonchak had a significantly higher content of Na (3.1%), probably indicating the existence of evaporites (i.e., NaCl and $Na_2SO_4 \cdot 10H_2O$), which was consistent with a previous study that identified the elemental ratios of the dissolved solutes in river water within the Lake Qinghai catchment (Jin et al., 2010a).

In this study, alpine frost desert soil and peat soil had a significantly higher content of trace elements, except Sr, which was possibly attributed to the weathering of rock. Further studies were needed to determine the reason for this enrichment.

3.3. Potential source identification by multivariate analyses

Cluster analysis was applied to the standardised data using War's method, with Euclidian distances as the criterion for the forming of clusters of elements (Han et al., 2006). In general, this form of CA was regarded as very efficient, although it tended to create small clusters. A dendrogram (cluster tree) for 15 elements was shown in Fig. 3. The elements can be classified into three major groups.

Group 1 Ca. Dominated by carbonate weathering with carbonate areas of 15,053.2 km^2, accounting for 59.6% of the catchment, which

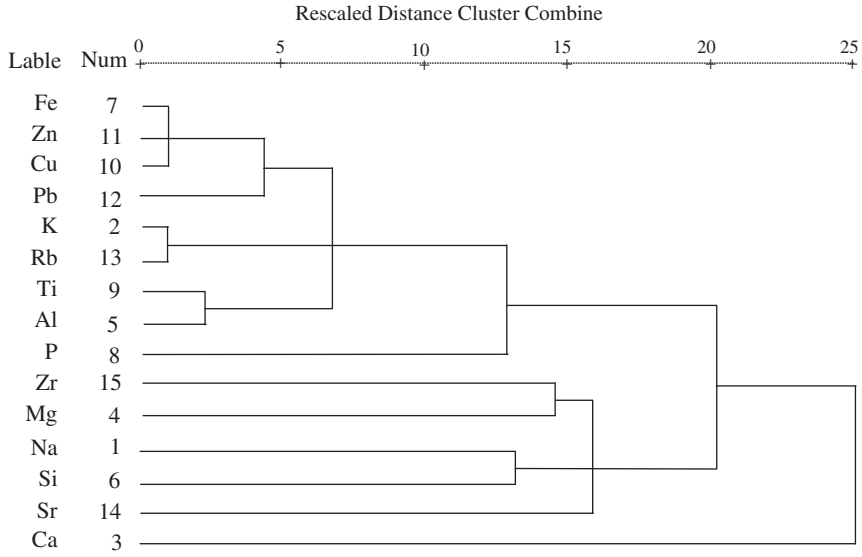

Fig. 3. Dendrogram of the cluster analysis of topsoil based on elements concentrations (n = 73).

further confirmed the importance of carbonate in the processes of rock weathering processes discussed above.

Group 2 Mg, Na, Si, Zr and Sr. They could have resulted from silicate weathering with silicate areas of 5296.2 km^2, accounting for 20.9% of the catchment. Natural silicate minerals contained Zr-bearing minerals (such as $ZrSiO_4$). Although elemental Sr was widely associated with carbonate, its presence in soil was also a consequence of silicate minerals weathering (Jacobson and Blum, 2000).

Group 3 Fe, Zn, Cu, Pb, K, Rb, Ti, Al and P. This group could be further subdivided into four subgroups: Fe–Zn–Cu–Pb: K–Rb; Ti–Al; and P. The first subgroup indicated that the trace elements Cu, Zn and Pb could considered to be siderophile elements. The second subgroup represented alkali metals. The third group represented the bedrock composition of soils. The final subgroup indicated the accumulation of P in topsoil, possibly from the litterfall of grasslands.

To further investigate the relationships between the elements, the principal component analysis was performed. PCA was used to extract quantitative information for the identification of the sources of pollutants (Han et al., 2006; Lu et al., 2010). Based on the loadings of the principal components (PCs) in Table 2, the 15 elements could be grouped into four PCs. The classification of the elements by PCA was consistent with the results from CA: PC1 from PCA and Group 3 from CA; PC2 and PC3 from PCA and Group 2 from CA, PC4 from PCA and Group 1 from CA. By comparison, Group 2 constituting of two subgroups (Mg, Na, Si, and Zr and Sr) was divided into PC2 (Mg–Na–Si) and PC3 (Zr–Sr), which indicate Zr-bearing or Sr-bearing minerals from the weathering of different silicate minerals in the rock weathering processes. In summary, four factors were obtained, accounting for 85.76% of the total variance. PC1 was dominated by Fe, Zn, Cu, Pb, K, Rb, Ti, Al and P, and accounted for 52.7% of the total variance. In this case, the P loadings (0.62) were not as high as the loadings of the other elements in the group, which may imply a quasi-independent behaviour within the group. This was consistent with the subgroup from CA, and confirmed that the topsoil/UCC ratio for P exceeded unity. PC2 was dominated by Na and Si, being produced by silicate, and accounted for 13.85% of the total variance. PC3 was dominated by Sr and Zr, and accounted for 10.87% of the total variance. PC4 was dominated by Ca, being produced by carbonate, and accounted for 8.2% of the total variance.

Table 2
Rotation component matrix of major and trace elements within the Lake Qinghai catchment.

Elements	Component loadings				Extraction
	PC1	PC2	PC3	PC4	
Na	−0.45	**0.61**	−0.34	−0.07	0.689
K	**0.94**	−0.24	0.08	0.02	0.948
Ca	0.06	−0.01	0.13	**0.88**	0.801
Mg	0.31	**0.71**	−0.42	0.16	0.807
Al	**0.84**	0.31	0.15	0.02	0.818
Si	0.12	**0.95**	−0.06	0.05	0.924
Fe	**0.95**	0.17	0.17	0.02	0.964
P	**0.62**	0.41	0.39	−0.01	0.700
Ti	**0.86**	0.23	0.32	0.17	0.928
Cu	**0.96**	0.08	0.04	−0.04	0.925
Zn	**0.97**	0.13	0.14	0.03	0.986
Pb	**0.92**	−0.19	0.15	0.10	0.907
Rb	**0.97**	0.04	0.15	−0.04	0.973
Sr	−0.33	0.09	**0.82**	0.05	0.794
Zr	0.20	0.06	**0.62**	0.52	0.700
Initial eigenvalues	7.905	2.078	1.632	1.249	
% variance	52.7	13.854	10.878	8.325	
Cumulative %	52.7	66.554	77.432	85.757	

Extraction method: principal component analysis.
Rotation method: Varimax with Kaiser normalisation. Rotation converged in 5 iterations.
Bold data: PCA loadings > 0.6.

3.4. The spatial distribution of trace elements by GIS mapping techniques

The geochemical mapping produced by GIS provided a reliable means of monitoring environmental conditions and identifying hotspots, especially for trace elements (Facchinelli et al., 2001; Li et al., 2004). Geochemical maps of the selected elements (including Cu, Zn, Pb, Rb, Sr, Zr, Ti and P) were shown in Fig. 4.

Three spatial patterns were apparent from the geochemical maps of the study area. First, the spatial distribution maps for Cu, Zn, Pb, Rb and Ti showed similar geographical trends, which corresponded to those of PC1 from PCA and Group 3 from CA discussed above, with high concentrations in the northeast (representing the coalfield), northwest (village and pastoral settlements) and west of lake (roadside settlements). The results indicate that human activities have had an influence on virgin topsoil in the Lake Qinghai catchment. Previous studies have indicated increased levels of trace elements in virgin soil in Qinghai–Tibet, due to anthropogenic activities such as such as mining (coal, potash and copper deposits) (Cao et al., 2011; Yang et al., 2013), over-grazing (Fan et al., 2010), land reclamation and cultivation (Jin et al., 2009), the Qinghai–Tibet railway (Qin and Zheng, 2010; Zhang et al., 2012), highway construction (Wu et al., 2003), tourism development (Wang et al., 2011) and others. Second, the spatial distributions of Sr and Zr corresponded to those of PC3 from PCA. High concentrations of both elements were found in the areas north and south of the lake, which could be due to differences in the natural distributions of Sr-bearing minerals (such as $SrSO_4$ or $SrCO_3$) and Zr-bearing minerals ($ZrSiO_4$) in the bedrock. Third, the spatial distribution of P revealed higher values in the central catchment that corresponded to grass cover in alpine meadow soil and alpine steppe soil (Fig. 1), and was consistent with the results of the multivariate analysis (CA and PCA) reported above and the ratio of P/UCC.

3.5. Implications of chemical weathering

The chemical index of alteration could qualitatively indicate the weathering intensity and weathering environment (Nesbitt and Young, 1982; Selvaraj and Chen, 2006). The *CIA* has been successfully applied in a large number of studies of topsoil and other depositional environments such as riverine solutes, lacustrine or ocean deposits, loess profiles and even ice sheets (Hren et al., 2007).

An Al_2O_3–$(CaO^* + Na_2O)$–K_2O diagram derived from the thermodynamic calculation of mineral stability and leaching experiments using feldspar could indicate the trends and changes of chemical weathering processes (Nesbitt and Young, 1984).

Fig. 5 was a mixing plot that was used to infer the weathering stage and environment based on the *CIA* index (panel on the right), as well as the weathering trends and processes on an A–CN–K diagram (panel on the left). The mean *CIA* value was recalculated as 64.5 (mean value) with a range from 57.2 (marsh solonchak) to 70.2 (alpine frost desert soil) in Lake Qinghai catchment, which indicated the primary stage of weathering, with the world average *CIA* value being 72.1 (Li and Yang, 2010). However, previous studies of weathering environments, based on statistical analyses, have suggested that *CIA* values of 50–65, 65–85 and 85–100 indicate cold-dry, warm-humid and heat-damp conditions, respectively (Selvaraj and Chen, 2006). The *CIA* mean value of 64.5 indicated that the chemical weathering environment was a cold-dry climate. In addition, the chemical composition of common shale in eastern China, which typically represents the product of the UCC weathering (Nesbitt and Young, 1982), was conceived as a final end-number (club symbol in Fig. 5) in a semi-arid area. The values for loess were considered to be a transition (diamond symbol in Fig. 5), and the UCC was considered to be the initial source (spade symbol in Fig. 5). The direction of the UCC toward terrigenous shale in the figure

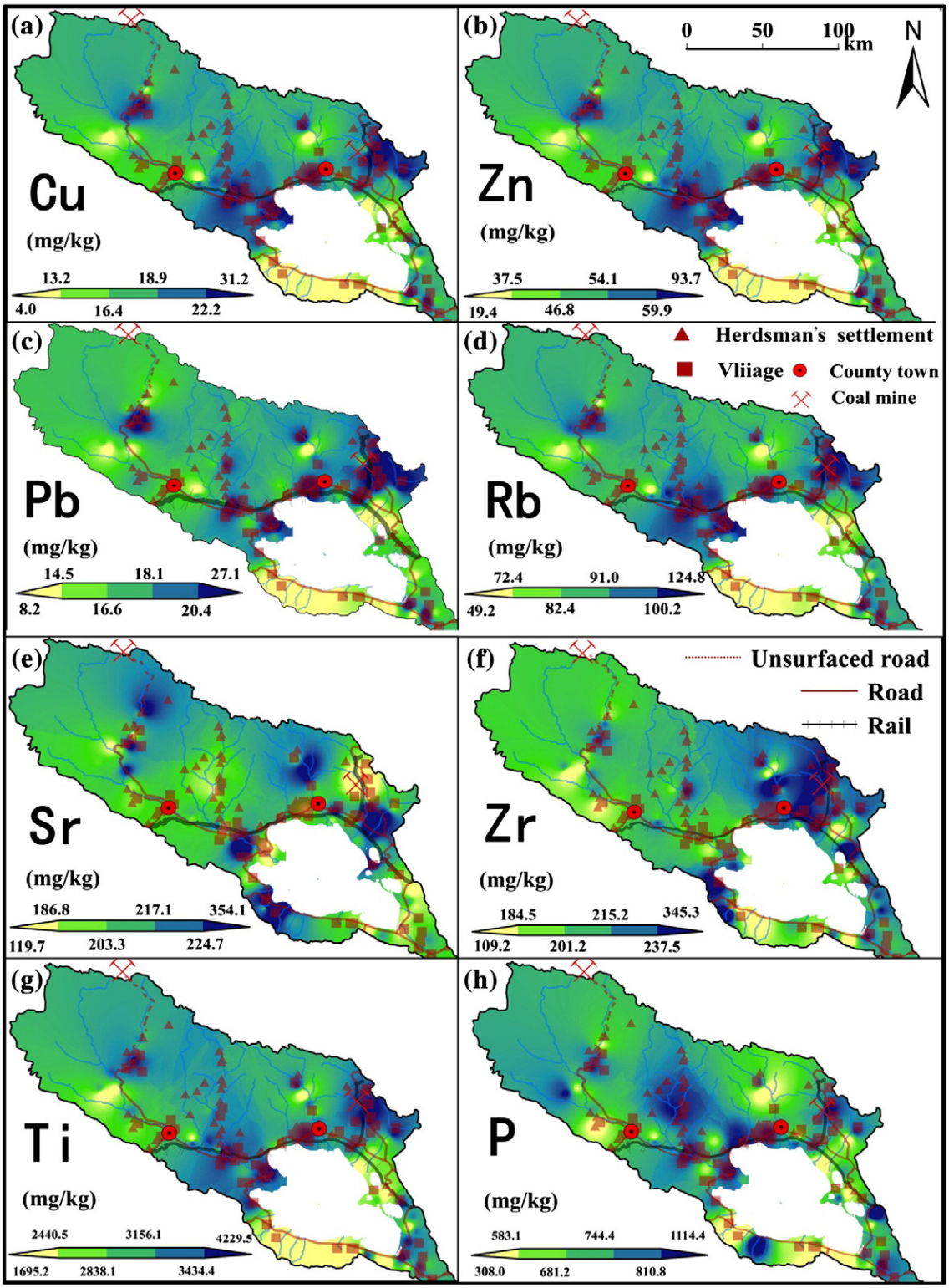

Fig. 4. Spatial distribution of Cu (a), Zn (b), Pb (c), Rb (d), Sr (e), Zr (f), Ti (g) and P (h), respectively, in topsoil within the Lake Qinghai catchment.

represents the weathering trend of the catchment. Finally, the main minerals (potassium feldspar, dolomite, illite, plagioclase, smectite, kaolinite, gibbsite) could also be projected on an A–CN–K diagram (Chi and Yan, 2007). The data points of the topsoil were parallel to the axes of the A–CN line and were located between plagioclase and smectite. The information on the A–CN–K diagram in Fig. 5 indicated that the products of weathering were smectite and plagioclase, with no kaolinite. In terms of the elemental geochemical signature, the effect of decalcification and the removal of Na (dissolution of plagioclase) on the topsoil was accompanied by the evolution of an Al enrichment. The chemical weathering of the semi-arid Lake Qinghai catchment was characterised by the carbonate control of the primary weathering stage under cold-dry climatic conditions and a transition between Ca and/or Na removal.

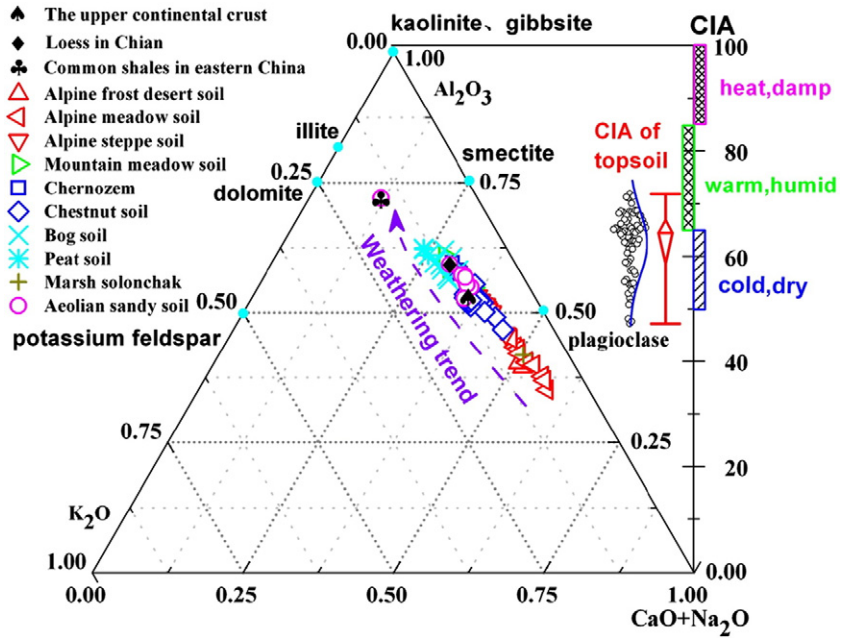

Fig. 5. Mixing plots between A–CN–K of topsoil chemical elements (the arrow indicating chemical weathering trend) and ranks/orders of *CIA* index indicating chemical weathering environment in topsoil within the Lake Qinghai catchment.

4. Conclusions

The soil types of the Lake Qinghai catchment can be divided into six soil orders and 10 soil groups. Enriched Ca levels were observed in alpine soil, pedocal, solonchak and aeolian sand soil. The high Na content of marsh solonchak indicates the possible presence of evaporites. The ratios of trace elements to the UCC indicated a deficit of Cu and Zn but an enrichment of Pb in the topsoil. The topsoil/UCC ratios of P exceeded unity, which indicated the accumulation of P in topsoil possibly from the litterfall of grasslands.

Soil geochemical patterns of the elements investigated suggested that they were derived from natural sources, as confirmed by the CA and PCA analyses, but there was some human influence on virgin topsoil in the Lake Qinghai catchment identified by GIS mapping.

Chemical weathering was characterised by a major carbonate control on the primary weathering stage under cold-dry climatic conditions, with Ca and/or Na removal.

Acknowledgements

This study was supported by the China Eleventh Five-year Plan Science and Technology Support Project (2012BAH31B03), and the National Basic Research Program of China (2010CB833403).

Appendix A. Supplementary data

Supplementary data to this article can be found online at http://dx.doi.org/10.1016/j.gexplo.2014.12.008.

References

Acosta, J.A., Faz, A., Martínez-Martínez, S., Zornoza, R., Carmona, D.M., Kabas, S., 2011. Multivariate statistical and GIS-based approach to evaluate heavy metals behavior in mine sites for future reclamation. J. Geochem. Explor. 109 (1–3), 8–17.

Almeida, M.D., Lacerda, L.D., Bastos, W.R., Herrmann, J.C., 2005. Mercury loss from soils following conversion from forest to pasture in Rondonia, Western Amazon. Brazil. Environ. Pollut. 137 (2), 179–186.

An, F., Ma, H., Wei, H., Lai, Z., 2012. Distinguishing aeolian signature from lacustrine sediments of the Qaidam Basin in northeastern Qinghai–Tibetan Plateau and its palaeoclimatic implications. Aeolian Res. 4, 17–30.

Angelone, M., Vaselli, O., Bini, C., Coradossi, N., 1993. Pedogeochemical evolution and trace-elements availability to plants in ophiolitic Soils. Sci. Total Environ. 129 (3), 291–309.

Baize, D., Sterckeman, T., 2001. Of the necessity of knowledge of the natural pedo-geochemical background content in the evaluation of the contamination of soils by trace elements. Sci. Total Environ. 264 (1–2), 127–139.

Baker, J.L., Campbell, K.I., Johnson, H.P., Hanway, L.L., 1975. Nitrate, phosphorus and sulphate in subsurface drainage water. J. Environ. Qual. 4 (3), 406–412.

Baveye, P.C., Rangel, D., Jacobson, A.R., Laba, M., Darnault, C., Otten, W., Radulovich, R., Camargo, F.A.O., 2011. From dust bowl to dust bowl: soils were still very much a frontier of science. Soil Sci. Soc. Am. J. 75 (6), 2037–2048.

Cao, J.J., An, Z.S., 2010. Introduction and progress of the project for technology integration and experimental demonstration of and environmental rehabilitation in Qinghai Lake Basin. J. Earth Environ. 3, 158–161 (in Chinese, with English Abstract).

Cao, W., Sheng, Y., Qin, Y., Li, J., Wu, J., 2011. An application of a new method in permafrost environment assessment of Muli mining area in Qinghai–Tibet Plateau, China. Environ. Earth Sci. 63 (3), 609–616.

Chen, J., An, Z., Liu, L., Ji, J., Yang, J., Chen, Y., 2001. Variations in chemical compositions of the eolian dust in Chinese Loess Plateau over the past 2.5 Ma and chemical weathering in the Asian inland. Sci. China Ser. D 44, 403–441.

Chi, Q., Yan, M., 2007. Handbook of Elemental Abundance for Applied Geochemistry. Geological Publishing House, Beijing, pp. 1–148 (in Chinese).

Dai, S., Ren, D., Chou, C.L., Finkelman, R.B., Seredin, V.V., Zhou, Y., 2012. Geochemistry of trace elements in Chinese coals: a review of abundances, genetic types, impacts on human health, and industrial utilization. Int. J. Coal Geol. 94, 3–21 (SI).

Diaz, R.V., Aldape, J., Flores, M., 2002. Identification of airborne particulate sources, of samples collected in Ticoman, Mexico, using PIXE and multivariate analysis. Nucl. Instrum. Methods Phys. Res. B Beam Interact. Mater. Atoms 189, 249–253.

Facchinelli, A., Sacchi, E., Mallen, L., 2001. Multivariate statistical and GIS-based approach to identify heavy metal sources in soils. Environ. Pollut. 114 (3), 313–324.

Fan, J.W., Shao, Q.Q., Liu, J.Y., Wang, J.B., Harris, W., Chen, Z.Q., Zhong, H.P., Xu, X.L., Liu, R.G., 2010. Assessment of effects of climate change and grazing activity on grassland yield in the Three Rivers Headwaters Region of Qinghai–Tibet Plateau, China. Environ. Monit. Assess. 170 (1–4), 571–584.

Goldich, S., Gast, P., 1996. Effects of weathering on the Rb–Sr and K–Ar ages of biotite from the Morton Gneiss, Minnesota. Earth Planet. Sci. Lett. 1 (6), 372–375.

Han, Y.M., Du, P.X., Cao, J.J., Posmentier, E.S., 2006. Multivariate analysis of heavy metal contamination in urban dusts of Xi'an, Central China. Sci. Total Environ. 355 (1–3), 176–186.

Han, Y., Cao, J., Posmentier, E.S., Fung, K., Tian, H., An, Z., 2008. Particulate-associated potentially harmful elements in urban road dusts in Xi'an, China. Appl. Geochem. 23 (4), 835–845.

Henderson, A.C.G., Holmes, J.A., 2009. Palaeolimnological evidence for environmental change over the past millennium from Lake Qinghai sediments: a review and future research prospective. Quat. Int. 194, 134–147.

Hren, M.T., Chamberlain, C.P., Hilley, G.E., Blisniuk, P.M., Bookhagen, B., 2007. Major ion chemistry of the Yarlung Tsangpo–Brahmaputra river: chemical weathering, erosion, and CO_2 consumption in the southern Tibetan plateau and eastern syntaxis of the Himalaya. Geochim. Cosmochim. Acta 71 (12), 2907–2935.

Huang, B., Gong, Z., 2005. Geochemical barriers and element retention in soils in different landscapes of the Tianshan Mountain area, Xinjiang, China. Geoderma 126 (3–4), 337–351.
Huang, B., Gong, Z., Gu, G., 2006. Elemental geochemistry of alto-cryic soils of Qinghai–Tibet Plateau in China — an example from the unpopulated Kekexili region. Geochem. J. 40 (2), 211–218.
ISSCAS (Institute of Soil Science, Chinese Academy of Sciences), 1978. Soil of China. Science Press, Beijing, pp. 5–36 (in Chinese).
IUSS Working Group WRB, 2006. World Reference Base for Soil Resources 2006. 2nd edition. World Soil Resources Reports No. 103FAO, Rome (http://www.fao.org/ag/agl/agll/wrb/doc/wrb2006final).
Jacobson, A.D., Blum, J.D., 2000. Ca/Sr and $^{87}Sr/^{86}Sr$ geochemistry of disseminated calcite in Himalayan silicate rocks from Nanga Parbat: influence on river-water chemistry. Geology 28 (5), 463–466.
Jin, Z., Han, Y., Chen, L., 2009. Past atmospheric Pb deposition in Lake Qinghai, northeastern Tibetan Plateau. J. Paleolimnol. 43 (3), 551–563.
Jin, Z., Wang, S., Zhang, F., Shi, Y., 2010a. Weathering, Sr fluxes, and controls on water chemistry in the Lake Qinghai catchment, NE Tibetan Plateau. Earth Surf. Process. Landf. 35 (9), 1057–1070.
Jin, Z., You, C.F., Wang, Y., Shi, Y., 2010b. Hydrological and solute budgets of Lake Qinghai, the largest lake on the Tibetan Plateau. Quat. Int. 218 (1–2), 151–156.
Kaiser, H.F., 1960. The application of electronic computers to factor analysis. Educ. Psychol. Meas. 20, 141–151.
Kleinman, P.J.A., Needelman, B.A., Sharpley, A.N., McDowell, R.W., 2003. Using soil phosphorus profile data to assess phosphorus leaching potential in manured soils. Soil Sci. Soc. Am. J. 67 (1), 215–224.
Korobova, E.M., Veldkamp, A., Ketner, P., Kroonenberg, S.B., 1997. Element partitioning in sediment, soil and vegetation in an alluvial terrace chronosequence, Limagne rift valley, France: a landscape geochemical study. Catena 31 (1–2), 91–117.
Larney, F.J., Izaurralde, R.C., Janzen, H.H., Olson, B.M., Solberg, E.D., Lindwall, C.W., Nyborg, M., 1995. Soil-erosion–crop productivity relationships for 6 Alberta soils. J. Soil Water Conserv. 50 (1), 87–91.
Li, C., Yang, S., 2010. Was chemical index of alteration (*CIA*) a reliable proxy for chemical weathering in global drainage basins? Am. J. Sci. 310 (2), 111–127.
Li, S., Zhang, Q., 2010. Spatial characterization of dissolved trace elements and heavy metals in the upper Han River (China) using multivariate statistical techniques. J. Hazard. Mater. 176 (1–3), 579–588.
Li, X.D., Poon, C.S., Liu, P.S., 2001. Heavy metal contamination of urban soils and street dusts in Hong Kong. Appl. Geochem. 16 (11–12), 1361–1368.
Li, X.D., Lee, S.L., Wong, S.C., Shi, W.Z., Thornton, L., 2004. The study of metal contamination in urban soils of Hong Kong using a GIS-based approach. Environ. Pollut. 129 (1), 113–124.
Li, X.Y., Xu, H.Y., Sun, Y.L., Zhang, D.S., Yang, Z.P., 2007. Lake-level change and water balance analysis at Lake Qinghai, west China during recent decades. Water Resour. Manag. 21 (9), 1505–1516.
Li, X.D., Wang, W.X., Zhu, Y.G., 2012. Trace metal pollution in China. Sci. Total Environ. 421, 1–2.
Li, Y., Gou, X., Wang, G., Zhang, Q., Su, Q., Xiao, G., 2008. Heavy metal contamination and source in arid agricultural soil in central Gansu Province, China. J. Environ. Sci. (China) 20 (5), 607–612.
Li, Z., Ma, Z., van der Kuijp, T.J., Yuan, Z., Huang, L., 2014. A review of soil heavy metal pollution from mines in China: pollution and health risk assessment. Sci. Total Environ. 468, 843–853.
LIGCAS (Lanzhou Institute of Geology of Chinese Academy of Sciences), 1979. A Synthetically Investigation Report on Qinghai Lake. Science Press, Beijing, pp. 1–270 (in Chinese).
LIGCAS (Lanzhou Institute of Geology of Chinese Academy of Sciences), 1994. Evolution of Recent Environment in Qinghai Lake and Its Prediction. Science Press, Beijing, pp. 1–343 (in Chinese).
Liu, C., 2009. Biogeochemical processes and cycling of nutrients in the earth's surface: cycling of nutrients in soil–plant systems of karstic environments, southwest China. Science Press, Beijing, pp. 1–38 (in Chinese).
Liu, G., Tao, L., Liu, X., Hou, J., Wang, A., Li, R., 2013. Heavy metal speciation and pollution of agricultural soils along Jishui River in non-ferrous metal mine area in Jiangxi Province, China. J. Geochem. Explor. 132, 156–163.
Loska, K., Wiechuła, D., 2003. Application of principal component analysis for the estimation of source of heavy metal contamination in surface sediments from the Rybnik Reservoir. Chemosphere 51 (8), 723–733.
Lottermoser, B.G., Ashley, P.M., Lawie, D.C., 1999. Environmental geochemistry of the Gulf Creek copper mine area, north-eastern New South Wales, Australia. Environ. Geol. 39 (1), 61–74.
Lu, X., Wang, L., Li, L.Y., Lei, K., Huang, L., Kang, D., 2010. Multivariate statistical analysis of heavy metals in street dust of Baoji, NW China. J. Hazard. Mater. 173 (1–3), 744–749.
Luo, X.S., Yu, S., Li, X.D., 2012a. The mobility, bioavailability, and human bioaccessibility of trace metals in urban soils of Hong Kong. Appl. Geochem. 27 (5), 995–1004.
Luo, X.S., Yu, S., Zhu, Y.G., Li, X.D., 2012b. Trace metal contamination in urban soils of China. Sci. Total Environ. 421, 17–30.
Ma, Y., 1997. Qinghai Soil. China Agriculture Press, Beijing, pp. 1–120 (in Chinese).
Mclennan, S.M., 1993. Weathering and global denudation. J. Geol. 101, 295–303.
Nesbitt, H., Young, G., 1982. Early Proterozoic climates and plate motions inferred from major element chemistry of lutites. Nature 299 (5885), 715–717.
Nesbitt, H.W., Young, G.M., 1984. Prediction of some weathering trends of plutonic and volcanic rocks based on thermodynamic and kinetic considerations. Geochim. Cosmochim. Acta 48 (7), 1523–1534.
Olorundare, O.F., Ipinmoroti, K.O., Popoola, A.V., Ayenimo, J.G., 2011. Anthropogenic influence on selected heavy metal contamination of urban soils of Akure City, Nigeria. Soil Sediment Contam. 20 (5), 509–524.
Peltola, P., Astrom, M., 2003. Urban geochemistry: a multimedia and multielement survey of a small town in northern Europe. Environ. Geochem. Health 25 (4), 397–419.
Qiang, M., Lang, L., Wang, Z., 2010. Do fine-grained components of loess indicate westerlies: insights from observations of dust storm deposits at Lenghu (Qaidam Basin, China). J. Arid Environ. 74 (10), 1232–1239.
Qin, Y., Zheng, B., 2010. The Qinghai–Tibet Railway: a landmark project and its subsequent environmental challenges. Environ. Dev. Sustain. 12 (5), 859–873.
Qiu, S.F., Zhu, Z.Y., Yang, T., Wu, Y., Bai, Y., Ouyang, T.P., 2014. Chemical weathering of monsoonal eastern China: implications from major elements of topsoil. J. Asian Earth Sci. 81, 77–90.
Selvaraj, K., Chen, C., 2006. Moderate chemical weathering of subtropical Taiwan: constraints from solid-phase geochemistry of sediments and sedimentary rocks. J. Geol. 114 (1), 101–116.
Shao, J., Yang, S., 2012. Does chemical index of alteration (*CIA*) reflect silicate weathering and monsoonal climate in the Changjiang River basin? Chin. Sci. Bull. 57 (10), 1178–1187.
Staff, S.S., 1999. Soil taxonomy: a basic system of soil classification for making and interpreting soil surveys. U.S. Department of Agriculture Handbook 2nd edition. Natural Resources Conservation Service, pp. 1–332.
Sun, G., Chen, Y., Bi, X., Yang, W., Chen, X., Zhang, B., Cui, Y., 2013. Geochemical assessment of agricultural soil: a case study in Songnen-Plain (Northeastern China). Catena 111, 56–63.
Suo, Y.R., C.L.T., C.C.G., 2000. The natural background value and characteristics of trace element in plants of the Qinghai Lake Region. Guangdong Trace Elem. Sci. 7 (6), 24–27 (in Chinese, with English Abstract).
Taylor, S.R., 1964. Abundance of chemical elements in the continental crust: a new table. Geochim. Cosmochim. Acta 28 (7), 1273–1285.
Teng, Y., Ni, S., Wang, J., Zuo, R., Yang, J., 2010. A geochemical survey of trace elements in agricultural and non-agricultural topsoil in Dexing area, China. J. Geochem. Explor. 104 (3), 118–127.
Wang, J., Tian, J., Li, X., Ma, Y., Yi, W., 2011. Evaluation of concordance between environment and economy in Qinghai Lake Watershed, Qinghai–Tibet Plateau. J. Geogr. Sci. 21 (5), 949–960.
Wang, H., Ma, M., Wang, X., Yuan, W., Song, Y., Tan, J., Huang, G., 2013. Seasonal variation of vegetation productivity over an alpine meadow in the Qinghai–Tibet Plateau in China: modeling the interactions of vegetation productivity, phenology, and the soil freeze–thaw process. Ecol. Res. 28 (2), 271–282.
Wei, B., Yang, L., 2010. A review of heavy metal contaminations in urban soils, urban road dusts and agricultural soils from China. Microchem. J. 94 (2), 99–107.
Wong, C.S.C., Li, X.D., 2004. Pb contamination and isotopic composition of urban soils in Hong Kong. Sci. Total Environ. 319 (1–3), 185–195.
Wu, Q., Shi, B., Liu, Y., 2003. Interaction study of permafrost and highway along Qinghai–Xizang Highway. Sci. China Ser. D Earth Sci. 46 (2), 97–105.
Xia, X., Yang, Z., Cui, Y., Li, Y., Hou, Q., Yu, T., 2013. Soil heavy metal concentrations and their typical input and output fluxes on the southern Song-nen Plain, Heilongjiang Province, China. J. Geochem. Explor. 139, 85–96 (SI).
Yang, T., Zhu, Z.Y., Gao, Q.Z., Rao, Z.G., Han, J.W., Wu, Y., 2010. Trace element geochemistry in topsoil from East China. Environ. Earth Sci. 60 (3), 623–631.
Yang, S., Zhang, H., Kong, M., Liu, Y., Liu, H., Xu, R., 2013. Study on surficial soil geochemistry in the high-elevation and frigid mountainous region: A case of Qulong porphyry copper deposit in Tibet. J. Geochem. Explor. 139, 144–151.
Ye, C., Li, S., Zhang, Y., Zhang, Q., 2011. Assessing soil heavy metal pollution in the water-level-fluctuation zone of the Three Gorges Reservoir, China. J. Hazard. Mater. 191 (1–3), 366–372.
Yu, J., Zhang, L., 2008. Lake Qinghai: Paleoenvironment and Paleoclimate. Science Press, Beijing, pp. 1–160.
Zhang, H., Wang, Z., Zhang, Y., Hu, Z., 2012. The effects of the Qinghai–Tibet railway on heavy metals enrichment in soils. Sci. Total Environ. 439, 240–248.
Zhao, X.R., Zhong, X.Y., Bao, H.J., Li, H.H., Li, G.T., Tuo, D.B., Lin, Q.M., Brookes, P.C., 2007. Relating soil P concentrations at which P movement occurs to soil properties in Chinese agricultural soils. Geoderma 142 (3–4), 237–244.